Pentylenetetrazole-induced Seizure Susceptibility in the Tau58/4 Transgenic Mouse Model of Tauopathy

Van Erum, Jan; Valkenburg, Femke; Van Dam, Debby; De Deyn, Peter Paul

Published in:
Neuroscience

DOI:
10.1016/j.neuroscience.2019.11.007

Publication date:
2020

Pentylenetetrazole-induced seizure susceptibility in the Tau58/4 transgenic mouse model of tauopathy

Jan Van Erum[1, ‡], Femke Valkenburg[1, ‡], Debby Van Dam[1,2], Peter Paul De Deyn[1,2,3,*]

[1] Laboratory of Neurochemistry and Behavior, Institute Born-Bunge, Department of Biomedical Sciences, University of Antwerp, Wilrijk (Antwerp), Belgium.

[2] Department of Neurology and Alzheimer Center, University of Groningen and University Medical Center Groningen (UMCG), Groningen, The Netherlands.

[3] Department of Neurology, Memory Clinic of Hospital Network Antwerp (ZNA) Middelheim and Hoge Beuken, Antwerp, Belgium

[‡] JVE and FV contributed equally on this manuscript

*Corresponding author.

(Peter Paul De Deyn)

Address: Campus Drie Eiken, Universiteitsplein 1, 2610 Wilrijk, Belgium

Email: p.p.de.deyn@umcg.nl

Tel: +32 32 65 26 20

Fax: +32 32 65 26 69

Abstract

In several tauopathies such as Alzheimer's disease (AD), an increased incidence of seizures is observed. Tau, one of the major proteins implicated in AD pathology, is an important regulator of neural network excitability and might participate in the underlying epileptic cascade. However, the mechanisms underlying this relationship are not fully elucidated. We aim to investigate this mechanism by analyzing seizure susceptibility to the convulsant pentylenetetrazole (PTZ) in a novel rodent tauopathy model. A single dose of PTZ was systemically injected in Tau58/4 transgenic mice. To investigate whether young and aged heterozygous (HET) mice exhibit a higher susceptibility to seizures in comparison with wild-type (WT) littermates, video EEG in combination with behavioral scoring according to a modified Racine scale was used. The employment of different dosage groups enabled us to characterize the dose range reliably inducing seizures. Here, we report an increased seizure susceptibility in young but not in old HET Tau58/4 mice. Young HET animals displayed more severe seizures and had a reduced latency to the first seizure compared to WTs. Also, age-related differences in susceptibility could be demonstrated for both genotypes. Identification and targeting of secondary diseases such as epilepsy, which aggravate dementia and lead to earlier institutionalization, is key. This study finds that tau pathology itself is sufficient to alter seizure susceptibility in a rodent model, indicating that the disease process is crucial in the emergence of epilepsy in patients with tauopathy.

Keywords

Tauopathies; Epilepsy; EEG; PTZ; Mouse models

Introduction

In tauopathies such as Alzheimer's disease (AD) (Amatniek et al., 2006;Scarmeas et al., 2009) and frontotemporal dementia with parkinsonism-17 (FTDP-17) (Sperfeld et al., 1999), an increased incidence of epilepsy compared to age-matched control individuals can be observed, suggesting a link between an increased susceptibility to seizures and tau pathology.

Various animal experiments previously focused on the effects of tau on hyperexcitability of the brain, although the focus was mainly directed at an ablation of tau and its potential beneficial effect for the treatment of epileptic disorders (DeVos et al., 2013;Holth et al., 2013). These studies indicated that tau could modulate excitability in the absence of Aβ pathology. In addition, the positive effects of genetic tau ablation on seizure susceptibility were likely to be a tau-mediated event rather than a developmentally regulated phenomenon as was demonstrated by delivery of antisense oligonucleotides. Therefore, tau is a noteworthy target for future disease-modifying drugs.

To gain more insight into the key mechanisms of clinically relevant pathologic alterations in tau, various transgenic animal models have been developed. Most of these models express a mutant variant of the human tau gene, sometimes in combination with other AD-relevant genes. Even in the absence of other mutated AD genes, different tauopathy-specific mouse models display highly heterogeneous phenotypes, probably as a result of different isoforms with different mutations being expressed under different promoters. For a detailed overview of the established mouse models with their limitations and advantages we kindly refer to Koss et al. (Koss et al., 2016) and the Alzforum Research Models website (https://www.alzforum.org/research-models).

In this study, we made use of the Tau58/4 transgenic mouse model, which expresses the human 4R/0N tau isoform that contains the point mutation of proline-to-serine in codon 301 (P301S) of the MAPT gene. This results in tau overexpression, hyperphosphorylation, misfolding and aggregation.

Overexpression of human tau is present from birth onwards in heterozygous animals. Histologically, expression of human tau can be observed in the spinal cord from the age of 2 months onwards. In the cerebrum, hyperphosphorylated tau arises at the level of the pons and frontal cortices at 3 months of age. NFT formation is observed at the age of 6 months with both AT8 and Gallyas staining. Originating from the pons, tau pathology progressively spreads over the cerebrum and cerebellum with aging. At 12 months, NFTs are diffusely present in the frontal cortex and the pons and also appear in the cerebellum, midbrain and parietal cerebral cortex. Subsequently, tau pathology spreads to thalamus and hypothalamus by 18 months of age (*Figure 1*). The model presents with age-dependent impairments in motor coordination and cognition (unpublished results by Valkenburg et al.).

Garcia-Cabrero et al., were among the first to investigate the link between seizure susceptibility and overexpression of various human mutant FTDP-17 tau proteins in a mouse model (García-Cabrero et al., 2013). They observed spontaneous seizure activity in the brain of homozygous FTDP-17 mutants aged 5 months or older and concluded that human FTDP-17 mutant tau expression in the brain is sufficient to cause epileptic activity. Moreover, compared to WT controls, the model displayed an age-related increased susceptibility for pentylenetetrazole (PTZ)-induced seizures at convulsive doses in mice aged 6 to 14 months. However, no increased PTZ sensitivity was observed in the younger age group (1-5 months). The effects on hyperexcitability caused by tau neuropathology have not yet been elucidated, but various animal experiments have suggested that the glutamatergic system as well as the GABAergic system might play a crucial role (Dabir et al., 2006;Levenga et al., 2013).

Here, we aimed to investigate whether tau overexpression and its pathological consequences influence the susceptibility to PTZ-induced seizures in the Tau58/4 mouse model. By evaluating age-related differences in susceptibility, we might unravel which stage of tau pathology, could be responsible for an increased seizure susceptibility. Additionally, we performed an initial

characterization of a glutamate transporter (GLT-1) in the model to scrutinize a possible mechanism underlying hyperexcitability.

Materials and methods

Tau58/4 transgenic mice

Tau 58/4 mice were generated in a hybrid C57BL/6 × DBA2 background, and mice were backcrossed to C57BL/6J mice to create a congenic line, as previously described (Yin et al., 2017). All mice were group-housed in standard mouse cages under conventional laboratory conditions, and individually housed from the day of electrode implantation onward with constant room temperature (22 ± 2°C), humidity level (55 ± 5%), 12h/12h day/night cycle (lights on at 8 a.m.). Food and water were supplied *ad libitum*. Custom primers (Biolegio, The Netherlands) were used for genotyping by PCR analysis performed on DNA extracted from ear punches, collected from mice aged 4 weeks. All experiments were carried out in compliance with the European Community Council Directive (2010/63/EU) and were approved by the Animal Ethics Committee of the University of Antwerp (ECD approval n° 2014–82).

Video EEG recording

Animals were implanted with electroencephalography (EEG) electrodes (E363/96/1.6, Plastics One Inc., Roanoke, U.S.A.) via stereotactic surgery, as previously described (Van Erum et al., 2019). Shortly, the animals were intraperitoneally anesthetized with a mixture of ketamine (100 mg/kg, Nimatek 10%, Eurovet Animal Health BV, Netherlands) and xylazine (20 mg/kg, Rompun 2%, Bayer, Germany), after which two active electrodes were placed over the frontal cortex, and two over the parietal cortex (coordinates from reference point Bregma: right frontal cortex: anteroposterior (AP) + 2.0 mm, mediolateral (ML) + 2.0 mm; left frontal cortex: AP + 2.0 mm, ML – 2.0 mm; right parietal cortex: AP – 2.0 mm, ML + 2.0 mm; left parietal cortex: AP – 2.0 mm, ML – 2.0 mm; ground electrode: AP – 4.90 mm, ML 0.0 mm; reference electrode: AP – 6.70 mm, ML 0.0 mm). The electrodes were fixed to the

skull with carboxylate cement (Durelon™, 3M ESPE S.A., Germany). The sockets were attached to an electrode pedestal (MS 363, Plastics One, Roanoke, U.S.A.) and the assembly was secured to the skull by carboxylate cement (Durelon™, 3M ESPE S.A., Germany). Postoperatively, animals were housed individually and carefully monitored for pain and distress. In addition, 0.05 mg/kg buprenorphine (Vetergesic®, 0.3 mg/mL, Ecuphar, Oostkamp, Belgium) was subcutaneously administered every 12 hours in a volume of 10 mL/kg for two days after surgery.

After a seven-day recovery period, the animals were coupled to a tethered 40-channel EEG headbox (Large EEG headbox, Schwarzer Ahns, Germany). Video EEG started with three hours of baseline EEG-recording. The first two hours served as habituation. During the final hour, the actual baseline EEG was recorded and behavior was scored according to a modified Racine scale (Van Erum et al., 2019) to ensure that the animals were free of epileptiform activity prior to seizure induction. The signal was sampled at a rate of 250 Hz and band-pass filtered between 0.5 and 30 Hz. Post-PTZ observations had a minimal duration of one hour and were terminated when both behavior and EEG activity normalized for at least 15 minutes, with a maximum duration of two hours. One day after the recordings took place, animals were sacrificed and brains were extracted, frozen at -40°C in 2-methylbutane on dry ice and stored at -80°C for further analyses.

Acute seizure induction with PTZ

For the induction of seizures, a single dose of PTZ (Sigma-Aldrich™, St. Louis, U.S.A.; purity ≥ 99%) was administered intraperitoneally according to a random dosing scheme. Five doses of PTZ were studied (10, 20, 40, 60, 80 mg/kg) in young adult (3-month-old) and aged (12-15-month-old) mice. Young adult mice do not show formation of neurofibrillary tangles (NFTs) and paired helical filaments (PHFs), in contrast to the old age group, in which NFTs and PHFs are diffusely present in the brain (unpublished results by Valkenburg et al.). The injection volume was 10 mL/kg. At least 8 animals were used per dose group/genotype/age. Fewer animals were used due to the lack of a desired response in the lowest

dose groups. The exact number of animals included can be found in the legend of the figures. In addition, a clear overview has been provided in *table 1*. Researchers were blinded to the treatment, genotype and age status of animals.

Seizure scoring analysis

For evaluation of seizures, animals were monitored both electrographically and behaviorally, as previously described (Van Erum et al., 2019). The BrainRT™ software (OSG BVBA, Rumst, Belgium) was used for both registration and analysis of the different EEG traces. A seizure was electrographically defined as high amplitude, rhythmic discharges representing a distinct EEG trace lasting for a minimum of five seconds. Epileptic events occurring within an interval of five seconds without the EEG returning to baseline are defined as belonging to the same event (Minkeviciene et al., 2009). All seizures were manually defined in the BrainRT™ program. Behavioral scoring of the observed seizures was done in accordance with previously published work, in which the Racine scale was uniquely modified for mice (Van Erum et al., 2019). It categorizes 8 stages of severity (from 0 to 7), and the higher the number, the more severe the seizure behavior.

Quantitative EEG

To evaluate the characteristics of the EEG after PTZ injection, we assessed the power spectrum of the EEG 1 hour before and after PTZ injection. The EEG data of 1 hour were divided into overlapping segments using periodic 2-s Hamming windows with 50% overlap, then the power spectral density (PSD) was computed using the pwelch method (Welch, 1967). The relative EEG power was calculated at six different frequency bands: delta (1–3 Hz), theta (4–7 Hz), $alpha_1$ (8–10 Hz), $alpha_2$ (11-13 Hz) and beta (14–20 Hz). For each band, the relative power was obtained. Relative power was calculated as the ratio of the absolute power in a frequency band to the total absolute power (1–35 Hz). All power spectra derived after PTZ injection were compared to baseline and were therefore expressed as a percentage of their baseline level (*Figure 5*).

Immunohistochemistry

Sagittal brain sections (5 μm, paraffin-embedded) of young and old Tau58/4 mice (3 WT + 3 HET) were cut for immunohistochemical staining. Antigen retrieval was performed in citrate buffer using the microwave heating technique. The sections were subsequently pre-incubated in methanol + 1 % H_2O_2 for 30 min. Then, slides were incubated at 4 °C overnight with primary antibody (GLT-1, 1:500, Polyclonal rabbit antibody, Synaptic Systems, Göttingen, Germany) in TBS + 1 % BSA. After washing, the sections were incubated with biotinylated goat anti-rabbit IgG (1:500, DAKO, E0432) at room temperature for 30 min. Next, sections were washed with TBS and were incubated in avidin-biotin-peroxidase complex (Vectastain ABC kit, Vector Laboratories, PK-6100, California, U.S.A.) for 30 min and visualized with 3, 3'-Diaminobenzidine (DAB, Sigma, D-5637). The sections were counterstained with hematoxyline and eosine, and mounted with mounting medium (Historal, Ral Diagnostics, Martillac, France).

Reverse transcription quantitative polymerase chain reaction (RT-qPCR)

Analysis of GLT-1 mRNA expression was performed in cortical tissue derived from animals that were not included into the susceptibility study. All analyses were performed on left hemispheric cortices (n = 30) from HET and WT animals aged 3, 6 and 12 months, according to Janssens et al (Janssens et al., 2019). In short, RNA extraction was performed using the RNeasy® Plus Universal Mini kit (Qiagen, Hilden, Germany) and on-column DNase treatment was performed using the RNase-free DNase set (Qiagen, Hilden, Germany) following the manufacturer's instructions. Reverse transcription was performed on 800 ng RNA, using the iScript cDNA Synthesis kit (Bio-Rad Laboratories, Hercules, CA, USA) in 20 μL reactions. To analyze expression, specific GLT-1 primers (5'- CATGCTCCTCATTCTCACAG-3' and 5'- TCTCATTCTATCCAGCAGCC-3') (Eising et al., 2017) were used. Reverse transcription quantitative PCR analyses were performed on the Applied Biosystems StepOnePlus instrument (Foster City, CA, USA), with automatic threshold settings. All analyses were carried out in 10 μL reactions

containing 5 µL of the Power SYBR Green Master Mix (Applied Biosystems, Foster City, CA, USA), 1.5 µL of each primer (250 nM final concentration) and 2 µL cDNA (8 ng). Normalized relative quantities (NRQs) of GLT-1 were calculated using the qbase+ software (version 3.1, Biogazelle), implementing an efficiency-corrected delta-delta Cq method (Hellemans et al., 2007). Glyceraldehyde-3-phosphate dehydrogenase (Gapdh) and beta-actin (Actb) were used as reference genes, as they proved to be the most stably expressed according to the geNorm algorithm.

Statistical analysis

All data (mean ± SD) were statistically evaluated by means of parametric methods. General effects of genotype and age were assessed using general linear models (GLM). Post-hoc, independent samples Student's *t*-test was employed to assess genotype- and age-related differences. Categorical data of maximum seizure severity was evaluated with the Fisher's Exact Test. Results were considered statistically significant for a value of $p < 0.05$. Statistical calculations were performed using SPSS 24 (IBM, SPSS Inc., Chicago, IL, U.S.A.).

Based on the results of five different dose groups, the ED_{50}-value and LD_{50}-value were determined by means of the probit regression model using SPSS 24, which uses the ratio of responders relative to the total number of included subjects. The ED_{50} value is the dose at which 50 % of the study population experienced seizure activity, and the LD_{50} value is the dose that was lethal for 50 % of the studied population.

Results

This experiment was designed to examine age-related differences in seizure susceptibility and severity to PTZ-induced seizures between HET and WT Tau58/4 mice. Induced seizures were evaluated both electrographically and behaviorally, leading to a detailed examination of EEG parameters and seizure severity-related behavioral parameters.

PTZ-induced seizure severity and susceptibility in young and old Tau58/4 mice

Analyses with GLM have indicated a significant effect of dose, age and genotype on mean seizure severity (dose: $F(4,143) = 111.336$; $p = 0.000$, age: $F(1,143) = 30.267$; $p = 0.000$, genotype: $F(1,143) = 13.053$; $p = 0.000$). As the interaction term between age and dose was also significant ($F(4,143) = 4.398$; $p = 0.002$), we concluded that the observed age effect was dependent on the dose. The interaction effect between genotype and dose was not significant. To gain a better understanding of where these differences were located, post-hoc t-tests were performed. Independent samples Student's *t*- tests revealed both genotype-related and age-related differences in mean (MeS) and maximum (MaxS) seizure severity (*Figure 2*). Both MeS ($t = -2.638$; $p = 0.034$) and MaxS ($p = 0.038$) were significantly higher in 3-month-old HET mice compared to their WT littermates in the 20 mg/kg dose group. In addition, MeS was significantly different between genotypes in the 80 mg/kg group ($t = -3.256$; $p = 0.014$) and borderline significant in the 60 mg/kg dose group ($t = -2.005$; $p = 0.05$). MaxS was also significantly higher in young HET mice upon administration of 60 mg/kg PTZ compared to WT controls ($p = 0.030$). No differences in severity were observed in the 40 mg/kg dose group, however, the total number of insults was significantly higher in this dose group ($t = -3.504$; $p = 0.003$) (*data not shown*). Hence, young HET animals had more severe seizures compared to WT littermates. Remarkably, no significant genotype-related differences were found in old animals. *Figure 2* shows age-related differences in MeS and MaxS for almost all dose groups, but differences only appeared significant in the 60 mg/kg dose group for both WT (MeS: $t = -4.302$; $p = 0.001$, MaxS: $p = 0.003$) and HET mice (MeS: $t = -2.512$; $p = 0.024$, MaxS: $p = 0.046$), and for the WT mice in the 20 mg/kg dose group (MeS: $t = -3.510$; $p = 0.006$, MaxS: $p = 0.016$). The MaxS was also significantly higher in old mice compared to young ones upon administration of 40 mg/kg PTZ for both genotypes (WT: $p = 0.001$, HET: $p = 0.035$). Seizure severity displayed a dose-dependent increase (MeS: $F(1,143) = 111.336$; $p = 0.000$).

The amount of time the animals spent in insult state was computed based on the ratio of the total insult time divided by the total recording time, multiplied by 3600 seconds. This computation encompasses an internal correction for the loss of post-PTZ observation time due to early occurrence of death and for short minor seizures. Analyses with GLM revealed that the time in insult state was significantly affected by age ($F(1,143) = 18.714$; $p = 0.000$) but not by genotype ($F(1,143) = 0.208$; $p = 0.649$). However, a significant interaction between the main factors (age x genotype) was observed ($F(1,143) = 5.211$; $p = 0.024$. Post-hoc Student's *t*-test revealed significant differences between 3-month-old HET and WT mice in the 80 mg/kg dose group, whereby HET animals spent more time in insult state than WT controls (t -2.154; $p = 0.049$). Furthermore, both young WT and HET mice spent less time in seizure state than old mice in the 40 mg/kg dose group (WT: $t = -2.927$; $p = 0.013$ HET: $t = -2.677$; $p = 0.017$). In the 60 mg/kg group this effect was only statistically significant in the WT group ($t = -4.554$; $p = 0.001$), but a similar trend could be observed in the HET group ($t = -1.837$; $p = 0.086$).
We also observed that the time spent in insult state in old HET animals was lower than in young HET animals after a dose of 80 mg/kg PTZ ($t = 2.260$; $p = 0.045$). Thus, young HET animals appeared to spend more time in insult state compared to WT littermates. The time spent in insult state also increased with age, indicating the age-related component in all dose groups. Finally, a dose-dependent increase of the time spent in insult state was demonstrated.

An increased sensitivity for young HET Tau58/4 was also apparent from the ED_{50} and LD_{50} curves (*Figure 3*). Young WT animals were least sensitive to PTZ with an ED_{50} and LD_{50} value of 28.7 mg/kg and 80.3 mg/kg respectively. The dose-response curve of young HET animals was shifted to the left, resulting in reduced ED_{50} and LD_{50} concentrations (20.0 and 63.2 mg/kg, respectively). The effective and lethal doses were similar for the old age group.

Latency to first electrographically defined seizure

For the assessment of differences in latency to first seizure, a fixed value of 7200 seconds was assigned to animals, not displaying electrographic seizure activity, since this was the maximum recording time for all animals. The GLM statistic revealed no main genotype effect ($F(1,143) = 3.688$; $p = 0.058$), but a significant interaction with dose (genotype x dose) ($F(4,143) = 4.418$; $p = 0.002$). A genotype-dependent difference in latency in 3-month-old mice was visible in the 80 mg/kg dose group ($t = 2.917$; $p = 0.020$). Counterintuitively, in that same dose group of 80 mg/kg, young HET mice experienced their first electrographically defined seizure significantly faster in comparison to old HET mice ($t = -3.619$; $p = 0.017$). This age difference in latency to the first PTZ-induced electrographic seizure was not observed in WT littermates for any of the doses studied. In the 20 mg/kg dose group, we also observed an age- and genotype-related effect. Old WT animals ($t = 4.170$; $p = 0.002$) and young HET animals ($t = 2.644$; $p = 0.033$) had a shorter latency than young WT animals. An inverse relation between dose levels and latency to first insult could be observed in *Figure 4*. The higher the dose of PTZ, the earlier the first insult appeared.

qEEG: differences in seizure manifestation between frontal and parietal cortices

Spectral power bands were also investigated using GLM analysis. No age effect could be demonstrated. Genotype had a significant effect on frontal $alpha_2$ power ($F(1,29) = 5.086$; $p = 0.032$). We observed a significant effect of dose on all spectral parameters ($p < 0.016$), except for parietal delta power. Also, the location of the electrode (frontal vs parietal) significantly influenced $alpha_1$ ($F(1,29) = 14.336$; $p = 0.001$), theta ($F(1,29) = 24.037$; $p = 0.000$) and delta ($F(1,29) = 78.355$; $p = 0.000$) power. In the theta and delta range, these location effects were also dependent on the administered dose (location x dose: theta: ($F(1,29) = 8.518$; $p = 0.000$, delta: ($F(1,29) = 42.466$; $p = 0.000$)).

Upon administration of 10 mg/kg PTZ, the relative power for all frequency bands corresponded to baseline conditions (100%). There were slight differences between frontal and parietal EEG spectra in the theta ($t = 3.862$; $p = 0.001$), delta ($t = -2.298$; $p = 0.034$) and alpha/delta ($t = 2.731$; $p = 0.014$) power

band (*Figure 5A*). However, when administering a dose of 40 mg/kg, a dose which induced severe seizures but which is never fatal to the animal, a drop in relative alpha and beta power and an increase in relative theta power were observed. Depending on the location of the electrode (frontal or parietal), delta power either increased or decreased, suggesting a difference in seizure manifestation between frontal and parietal regions. Generally, differences between frontal and parietal spectra highly increased in the $alpha_1$ (t = 3.596; p = 0.002), theta (t = 3.384; p = 0.003), delta (t = -9.083; p = 3.8E-8), alpha/delta (t = 5.642; p = 2.4E-5) and alpha/(delta+theta) (t = 4.520; p = 2.65E-4) power band after a high dose of PTZ (*Figure 5B*). No genotype-related differences were found upon administration of a high dose, except for the frontal $alpha_2$ power in older animals, (t = 2.874; p = 0.021), which was significantly reduced in HET animals compared to WT littermates (*Figure 5C*).

GLT-1 immunohistochemistry in frontal cortex

By means of immunohistochemistry (IHC) we tried to elaborate whether the differences in PTZ susceptibility could be due to an altered expression of the glutamate transporter GLT-1. We observed scarcer immunoreactivity in the frontal cortical region of young HET mice compared to WT littermates (*Figure 6*). However, RT-qPCR analyses did not demonstrate significantly lower GLT-1 mRNA levels in the cortex of young HET mice (*Figure 7*), although a trend was observed. Of note, the RT-qPCR was performed on hemispheric cortices, and might explain the discrepancy between the IHC and RT-qPCR results. However, the frontal region was not investigated separately due to expected difficulties with limited sample availability. Immunoreactivity in old animals was similar to that in young HET mice. No genotype differences were observed at old age.

Discussion

In this study, no significant differences could be demonstrated between HET and WT animals at older ages, opposite to the study of Garcia-Cabrero et al. (García-Cabrero et al., 2013). In contrast, genotype-related differences in seizure susceptibility were found in the young group of three months of age. Our

findings thereby suggest that the presence of overexpressed, mutant hyperphosphorylated human tau alone is sufficient to cause heightened PTZ-induced seizure susceptibility. For both genotypes, an age-related effect was observed. Old animals were generally more susceptible for chemically induced seizures than young animals. Since both genotypes were affected, this age effect cannot be explained by the worsening of tau pathology solely.

Behavioral seizure severity is increased in young but not in old Tau58/4 mice when comparing to wild-type littermates

The single-dose systemic PTZ model reliably evoked seizures that increased in severity in a dose-dependent manner. By use of this model, we showed that young Tau58/4 HET mice in multiple dose groups experienced more severe seizures after administration of a single dose of PTZ compared to young WT controls. In the 40 mg/kg dose group, no genotype-related differences in seizure severity were observed. However, young HET mice seemed to have a higher total number of insults in this dose group, while no significant differences in mean seizure duration could be demonstrated (data not shown). Therefore, seizures probably also manifested more severely in HET animals in this dose group. Correspondingly, the ED_{50} and LD_{50} concentrations in young HET animals were markedly reduced compared to the age-matched WT controls. Counterintuitively, no genotype-related differences were present in the aged test group. Hence, our findings indicate that NFTs and PHFs (advanced stages of tauopathy) had no effect on seizure susceptibility in our model. Nonetheless, the possibility exists that aging effects in these mice masked genotype differences, since old mice were also significantly more susceptible to PTZ-induced seizures than young adults in the WT group.

The molecular mechanisms underlying the effects of tau on hyperexcitability have not yet been elucidated. The inhibitory neurotransmitter GABA might play a role in the development of hyperexcitability in tau pathology. In 2013, Levenga et al., demonstrated that the number of GABAergic neurons was decreased in the hippocampus of aged tau-mutant JNPL3 mice compared to controls

(Levenga et al., 2013). Moreover, hyperphosphorylated tau itself could also be of importance in the regulation of excitability and synchronization of neural networks (Holth et al., 2013). Tau enables the Fyn kinase to facilitate NMDA-elicited currents postsynaptically and thereby elicits hyperexcitability (Mondragon-Rodriguez et al., 2012).

Abnormally phosphorylated, ubiquitinated and filamentous tau in astrocytes resulted in a reduced expression of glutamate transporters, reducing the reuptake of glutamate at the level of the synaptic cleft (Dabir et al., 2006), possibly eliciting hyperexcitability. In PS19 mice, regional changes in glutamate levels correlated with tau pathology, synapse and neuron loss (Crescenzi et al., 2014). In our study, GLT-1 immunoreactivity appeared to be decreased in the frontal cortex of young HET Tau58/4 mice, a region in which the first pathological features arise. However, the qPCR analysis of cortical GLT-1 expression levels remained inconclusive. A study that involved the use of another P301S mouse model demonstrated reduced expression of GLT-1 in the superficial cortex of mice age 3 and 5 months (Sidoryk-Wegrzynowicz et al., 2017). Latter study specifically focused on astrocytic GLT-1 expression, although transgenic mutant tau was only present in neurons and not in astrocytes. This suggests the presence of a crosstalk between neurons and astrocytes, in which neuronal dysfunction drives the changes in astrocytic glutamate homeostasis. The influence that neurons exert on astrocytic function is poorly understood. A recent study has shown that neuron-derived signals may be key in upregulating gene expression and function of glutamate transporters in astrocytes (Hasel et al., 2017). It appears that GLT-1, either of astrocytic or neuronal nature, can become affected by neuronal tau pathology. Therefore, reduced expression of GLT-1 transporters, due to the presence of mutant human tau, might underlie the heightened PTZ-induced seizure susceptibility at a young age in the Tau58/4 model.

Additionally, increased mitochondrial stress is frequently associated with both epilepsy and tauopathies, and might fulfill a common pathologic role in seizure onset (Lasagna-Reeves et al., 2011;Liang and Patel, 2004). However, many more mechanisms might be involved. Therefore, in-depth

analysis of the molecular processes (e.g., transcriptome analysis (Janssen et al., 2017)) occurring in our model at different ages is a suited follow-up for this study.

The observed age effects are supported by others who have investigated the effects of acute seizures in the aged brain. These were thoroughly reviewed by Kelly et al (Kelly, 2010). In addition, aged C57BL/6J mice develop 'patient-like' hippocampal granular deposits (Krass et al., 2003), and display loss of certain neuronal populations (GABAergic interneurons) (Sugama et al., 2003), possibly contributing to these results. It would be interesting to address the observed aging effects in future studies by inclusion of true aging models (e.g., D-galactose-induced brain aging models (Sadigh-Eteghad et al., 2017)) to disentangle the influence of aging on seizure susceptibility.

The observation that the time spent in insult state is significantly lower in old HET animals than in young HET animals upon administration of 80 mg/kg is probably due to the increased latency to seizures demonstrated in older animals. In this dose group, all animals suffer from a premature death. By extending the latency to the first deadly insult, the older animals therefore appear to be less long in insult state given the time until death is comparable for all animals.

Latency to first insult is reduced in young Tau58/4 mice in the highest dose group

With increasing doses, the latency to the first insult was reduced. In the 80 mg/kg group, young HET had a decreased latency to the onset of the first seizure, thereby confirming again the increased sensitivity of young HET Tau58/4 mice to PTZ-induced seizures. Remarkably, the latency in these young HET animals was significantly shorter than in old HET mice. Although not reported, this effect could also be observed by Garcia-Cabrero et al., providing a substantial basis for a distinct underlying molecular process (García-Cabrero et al., 2013). DeVos et al. observed an inverse correlation between the latency to reach a seizure of stage 8 (= death) and the amount of endogenous tau protein in brain homogenate measured. Mice with higher levels of endogenous tau progressed to severe seizures more

quickly than those with lower endogenous tau levels (DeVos et al., 2013). The reduction of endogenous tau in hAPP mice also protected against behavioral deficits and excitotoxicity (Roberson et al., 2007), thereby stressing the importance of endogenous tau in neurological processes. Brion et al., observed that, during development, endogenous murine tau gradually decreased in cell bodies and dendrites, while human transgenic tau remained abundant (Brion et al., 1999). Although no alterations in the production of endogenous tau during aging are present in our mouse model, the proportion of endogenous tau to mutant human tau shifts during the aging process, thus possibly influencing the physiological function of murine tau. Since age-related differences in latency were only observed in the HET group, but not in the WT group, the effects were probably due to molecular effects resulting from advanced stages of tauopathy.

qEEG reveals differences in seizure manifestation between frontal and parietal cortices

To the best of our knowledge, this was the first time the effects on brain rhythms after PTZ injection were studied in mice via qEEG. We observed that after a high dose of PTZ (40 mg/kg), which induces severe but non-lethal convulsions, fast rhythms (alpha and beta) decreased, while slow rhythms (theta) prevailed. EEG and intracranial EEG studies have recorded abnormal slow-wave activity in patients with seizure-induced dysfunctions, both in the ictal (Englot et al., 2010) and post-ictal (Jan et al., 2001) period. During the post-ictal phase the brain recovers from the trauma induced by seizures, and this stage is often associated with behavioral changes, such as a loss in responsiveness and unconsciousness (Englot et al., 2010). Since mice were significantly more immobile after a high dose of PTZ, the increased cortical slowing could be linked to impaired consciousness/responsiveness. After administration of a high dose, differences between frontal and parietal regions augmented, suggesting an uncoupling between the regions and indicating that PTZ might have differential effects on different brain regions. Enhanced synchronization of slow oscillations in the parietal cortex are normally caused by simultaneous activity of large populations of cortical neurons (Bellesi et al., 2014). However, synchronization in epilepsy is a complex phenomenon and may appear different depending on the

spatial scale, the definition of synchrony and the signals being measured (Jiruska et al., 2013). PTZ is a GABAA receptor antagonist that induces generalized seizures after systemic injection. Physiologically, GABAergic inhibition enables synchronization of activity in cortical networks and contributes to the generation of a variety of brain activity patterns. The effects of the loss of GABA signaling on synchronicity are not yet understood. With studies to come, it would be interesting to assess the neuronal responses of GABA antagonism in vitro and in vivo. Hence, the processes underlying the focal slow activity in the parietal cortex remain a matter of conjecture.

Genotype-related differences in relative alpha power could only be demonstrated in old animals in the frontal area, but not in young animals, thereby suggesting that the power differences are not related to seizure severity. Possibly, differences in cortical neuronal physiology (e.g., synaptic/neuronal loss) or seizure manifestation due to the presence of tau pathology are responsible.

Conclusively, we investigated seizure susceptibility in a novel tauopathy mouse model. Our experiments indicate that seizures can be reliably evoked by PTZ, and that genotype differences in susceptibility occur in pre-NFT stages, indicating a role of pre-fibrillar hyperphosphorylated tau. The reported characterization of the Tau58/4 model enables more in-depth molecular investigations of seizure susceptibility mechanisms, as well as the use of the mouse model in research of therapeutic convulsion-reducing interventions.

Highlights
- Young Tau58/4 mice experience more severe PTZ-induced seizures than wild-type littermates, and also display a reduced latency to the first seizure. - Old Tau58/4 mice displayed no differences in seizure susceptibility compared to wild-type controls, despite diffuse presence of advanced tauopathy. - All mice, regardless of genotype, were more susceptible for seizures at older ages. - PTZ affects frontal and parietal EEG power spectra in a different manner.

Disclosures

None of the authors has any conflict of interest to disclose. We confirm that we have read the Journal's position on issues involved in ethical publication and affirm that this report is consistent with those guidelines.

Acknowledgements

This work was financed by the Interuniversity Poles of Attraction (IAP Network P7/16) of the Belgian Federal Science Policy Office, the Research Foundation – Flanders, the agreement between Institute Born-Bunge and the University of Antwerp, the Medical Research Foundation Antwerp, the Thomas Riellaerts research fund, and Neurosearch Antwerp, and Rotary International's 'Hope in Head'. The authors have no conflict of interest to declare. Special thanks go to Elke Calus and Jill Luyckx for the aid in behavioral scoring and to Tinne Koninckx and Inge Bats for histological preparations and photomicrographs. Jana Janssens performed the RT-qPCR experiments.

References

Amatniek JC, Hauser WA, DelCastillo-Castaneda C, Jacobs DM, Marder K, Bell K, Albert M, Brandt J, et al. (2006), Incidence and predictors of seizures in patients with Alzheimer's disease. Epilepsia 47:867-872.

Bellesi M, Riedner BA, Garcia-Molina GN, Cirelli C, Tononi G (2014), Enhancement of sleep slow waves: underlying mechanisms and practical consequences. Front Syst Neurosci 8:208-208.

Brion JP, Tremp G, Octave JN (1999), Transgenic expression of the shortest human tau affects its compartmentalization and its phosphorylation as in the pretangle stage of Alzheimer's disease. The American journal of pathology 154:255-270.

Crescenzi R, DeBrosse C, Nanga RPR, Reddy S, Haris M, Hariharan H, Iba M, Lee VMY, et al. (2014), In vivo measurement of glutamate loss is associated with synapse loss in a mouse model of tauopathy. NeuroImage 101:185-192.

Dabir DV, Robinson MB, Swanson E, Zhang B, Trojanowski JQ, Lee VM, Forman MS (2006), Impaired glutamate transport in a mouse model of tau pathology in astrocytes. The Journal of neuroscience : the official journal of the Society for Neuroscience 26:644-654.

DeVos SL, Goncharoff DK, Chen G, Kebodeaux CS, Yamada K, Stewart FR, Schuler DR, Maloney SE, et al. (2013), Antisense reduction of tau in adult mice protects against seizures. The Journal of neuroscience : the official journal of the Society for Neuroscience 33:12887-12897.

Eising E, Balog J, Ferrari MD, Datson NA, van den Maagdenberg AMJM (2017) Epigenetic signatures of migraine genes in a transgenic mouse model of familial hemiplegic migraine. Leiden: University of Leiden.

Englot DJ, Yang L, Hamid H, Danielson N, Bai X, Marfeo A, Yu L, Gordon A, et al. (2010), Impaired consciousness in temporal lobe seizures: role of cortical slow activity. Brain : a journal of neurology 133:3764-3777.

García-Cabrero AM, Guerrero-López R, Giráldez BG, Llorens-Martín M, Ávila J, Serratosa JM, Sánchez MP (2013), Hyperexcitability and epileptic seizures in a model of frontotemporal dementia. Neurobiology of Disease 58:200-208.

Hasel P, Dando O, Jiwaji Z, Baxter P, Todd AC, Heron S, Márkus NM, McQueen J, et al. (2017), Neurons and neuronal activity control gene expression in astrocytes to regulate their development and metabolism. Nature Communications 8:15132.

Hellemans J, Mortier G, De Paepe A, Speleman F, Vandesompele J (2007), qBase relative quantification framework and software for management and automated analysis of real-time quantitative PCR data. Genome Biology 8:R19.

Holth JK, Bomben VC, Reed JG, Inoue T, Younkin L, Younkin SG, Pautler RG, Botas J, et al. (2013), Tau loss attenuates neuronal network hyperexcitability in mouse and Drosophila genetic models of epilepsy. The Journal of neuroscience : the official journal of the Society for Neuroscience 33:1651-1659.

Jan MM, Sadler M, Rahey SR (2001), Lateralized postictal EEG delta predicts the side of seizure surgery in temporal lobe epilepsy. Epilepsia 42:402-405.

Janssen L, Dubbelaar ML, Holtman IR, de Boer-Bergsma J, Eggen BJ, Boddeke HW, De Deyn PP, Van Dam D (2017), Aging, microglia and cytoskeletal regulation are key factors in the pathological evolution of the APP23 mouse model for Alzheimer's disease. Biochimica et biophysica acta 1863:395-405.

Janssens J, Crans RAJ, Van Craenenbroeck K, Vandesompele J, Stove CP, Van Dam D, De Deyn PP (2019), Evaluating the applicability of mouse SINEs as an alternative normalization approach for RT-qPCR in brain tissue of the APP23 model for Alzheimer’s disease. Journal of Neuroscience Methods 320:128-137.

Jiruska P, de Curtis M, Jefferys JG, Schevon CA, Schiff SJ, Schindler K (2013), Synchronization and desynchronization in epilepsy: controversies and hypotheses. The Journal of physiology 591:787-797.

Kelly KM (2010), Aging models of acute seizures and epilepsy. Epilepsy Curr 10:15-20.

Koss DJ, Robinson L, Drever BD, Plucinska K, Stoppelkamp S, Veselcic P, Riedel G, Platt B (2016), Mutant Tau knock-in mice display frontotemporal dementia relevant behaviour and histopathology. Neurobiol Dis 91:105-123.
Krass KL, Colinayo V, Ghazalpour A, Vinters HV, Lusis AJ, Drake TA (2003), Genetic loci contributing to age-related hippocampal lesions in mice. Neurobiol Dis 13:102-108.
Lasagna-Reeves CA, Castillo-Carranza DL, Sengupta U, Clos AL, Jackson GR, Kayed R (2011), Tau oligomers impair memory and induce synaptic and mitochondrial dysfunction in wild-type mice. Molecular Neurodegeneration 6:39.
Levenga J, Krishnamurthy P, Rajamohamedsait H, Wong H, Franke TF, Cain P, Sigurdsson EM, Hoeffer CA (2013), Tau pathology induces loss of GABAergic interneurons leading to altered synaptic plasticity and behavioral impairments. Acta Neuropathologica Communications 1:34-34.
Liang LP, Patel M (2004), Mitochondrial oxidative stress and increased seizure susceptibility in Sod2(-/+) mice. Free radical biology & medicine 36:542-554.
Minkeviciene R, Rheims S, Dobszay MB, Zilberter M, Hartikainen J, Fulop L, Penke B, Zilberter Y, et al. (2009), Amyloid beta-induced neuronal hyperexcitability triggers progressive epilepsy. The Journal of neuroscience : the official journal of the Society for Neuroscience 29:3453-3462.
Mondragon-Rodriguez S, Trillaud-Doppia E, Dudilot A, Bourgeois C, Lauzon M, Leclerc N, Boehm J (2012), Interaction of endogenous tau protein with synaptic proteins is regulated by N-methyl-D-aspartate receptor-dependent tau phosphorylation. The Journal of biological chemistry 287:32040-32053.
Roberson ED, Scearce-Levie K, Palop JJ, Yan F, Cheng IH, Wu T, Gerstein H, Yu GQ, et al. (2007), Reducing endogenous tau ameliorates amyloid beta-induced deficits in an Alzheimer's disease mouse model. Science (New York, NY) 316:750-754.
Sadigh-Eteghad S, Majdi A, McCann SK, Mahmoudi J, Vafaee MS, Macleod MR (2017), D-galactose-induced brain ageing model: A systematic review and meta-analysis on cognitive outcomes and oxidative stress indices. PloS one 12:e0184122-e0184122.
Scarmeas N, Honig LS, Choi H, Cantero J, Brandt J, Blacker D, Albert M, Amatniek JC, et al. (2009), Seizures in Alzheimer disease: who, when, and how common? Arch Neurol 66:992-997.
Sidoryk-Wegrzynowicz M, Gerber YN, Ries M, Sastre M, Tolkovsky AM, Spillantini MG (2017), Astrocytes in mouse models of tauopathies acquire early deficits and lose neurosupportive functions. Acta Neuropathologica Communications 5:89.
Sperfeld AD, Collatz MB, Baier H, Palmbach M, Storch A, Schwarz J, Tatsch K, Reske S, et al. (1999), FTDP-17: an early-onset phenotype with parkinsonism and epileptic seizures caused by a novel mutation. Annals of neurology 46:708-715.
Sugama S, Yang L, Cho BP, DeGiorgio LA, Lorenzl S, Albers DS, Beal MF, Volpe BT, et al. (2003), Age-related microglial activation in 1-methyl-4-phenyl-1,2,3,6-tetrahydropyridine (MPTP)-induced dopaminergic neurodegeneration in C57BL/6 mice. Brain research 964:288-294.
Van Erum J, Van Dam D, De Deyn PP (2019), PTZ-induced seizures in mice require a revised Racine scale. Epilepsy & Behavior 95:51-55.
Welch P (1967), The use of fast Fourier transform for the estimation of power spectra: A method based on time averaging over short, modified periodograms. IEEE Transactions on Audio and Electroacoustics 15:70-73.
Yin Z, Valkenburg F, Hornix BE, Mantingh-Otter I, Zhou X, Mari M, Reggiori F, Van Dam D, et al. (2017), Progressive Motor Deficit is Mediated by the Denervation of Neuromuscular Junctions and Axonal Degeneration in Transgenic Mice Expressing Mutant (P301S) Tau Protein. Journal of Alzheimer's disease : JAD 60:S41-s57.

Figures

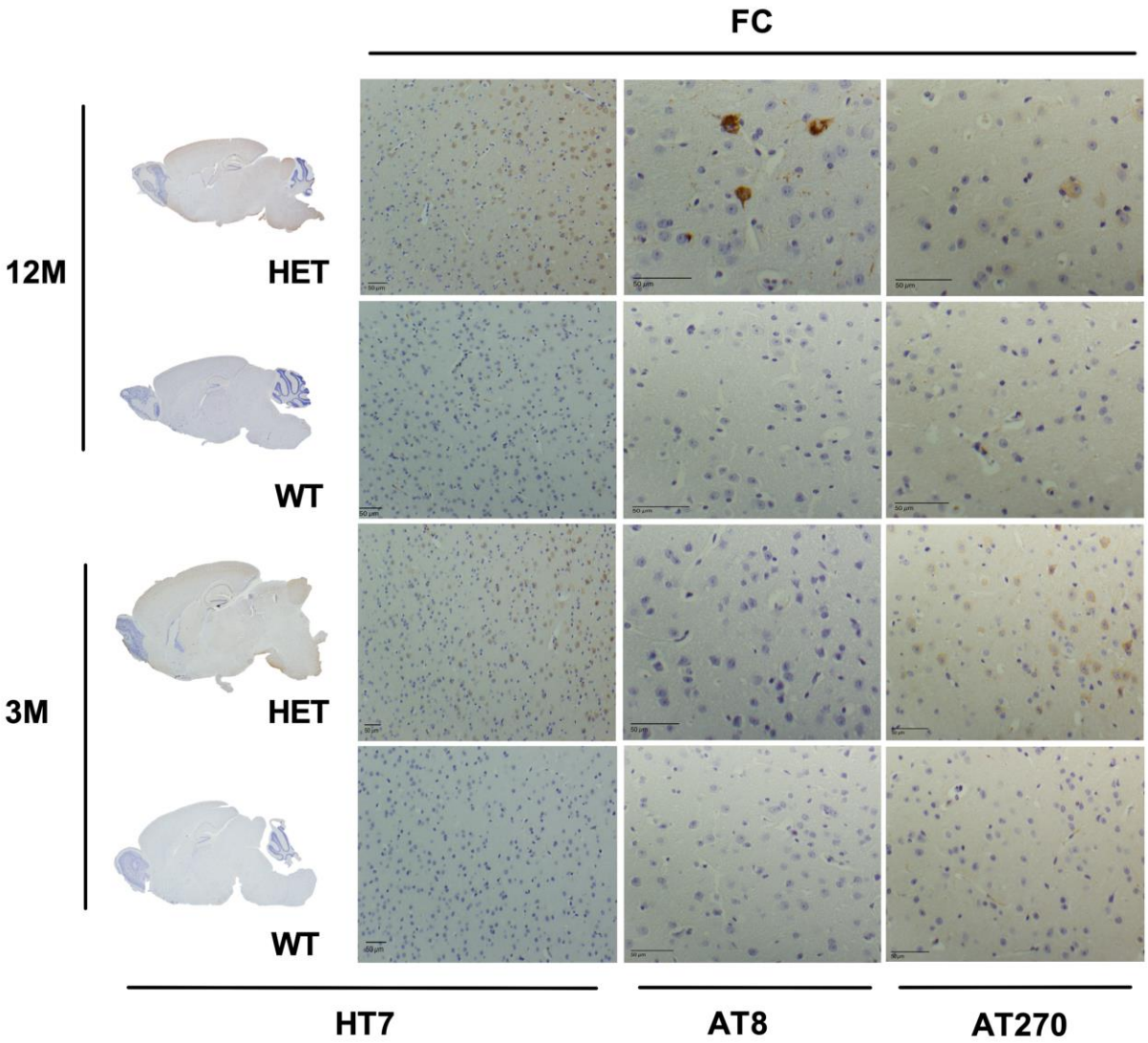

Figure 1. **Immunohistochemical staining of the brain of WT and HET Tau58/4 mice**. Here, HT7 antibody (whole saggital brain section and frontal cortex (FC)) stains human tau, while AT8 (frontal cortex) and AT270 (frontal cortex) antibodies stain phosho-tau epitopes. At 3 months of age, mutant human tau expression has resulted in AT270-positive tau proteins in the FC. No AT8-positive neurofibrillary tangles (NFTs) were observed at this stage. At 12 months, NFT pathology is diffusely present in the frontal cortex. HET=heterozygote; WT=wild-type.

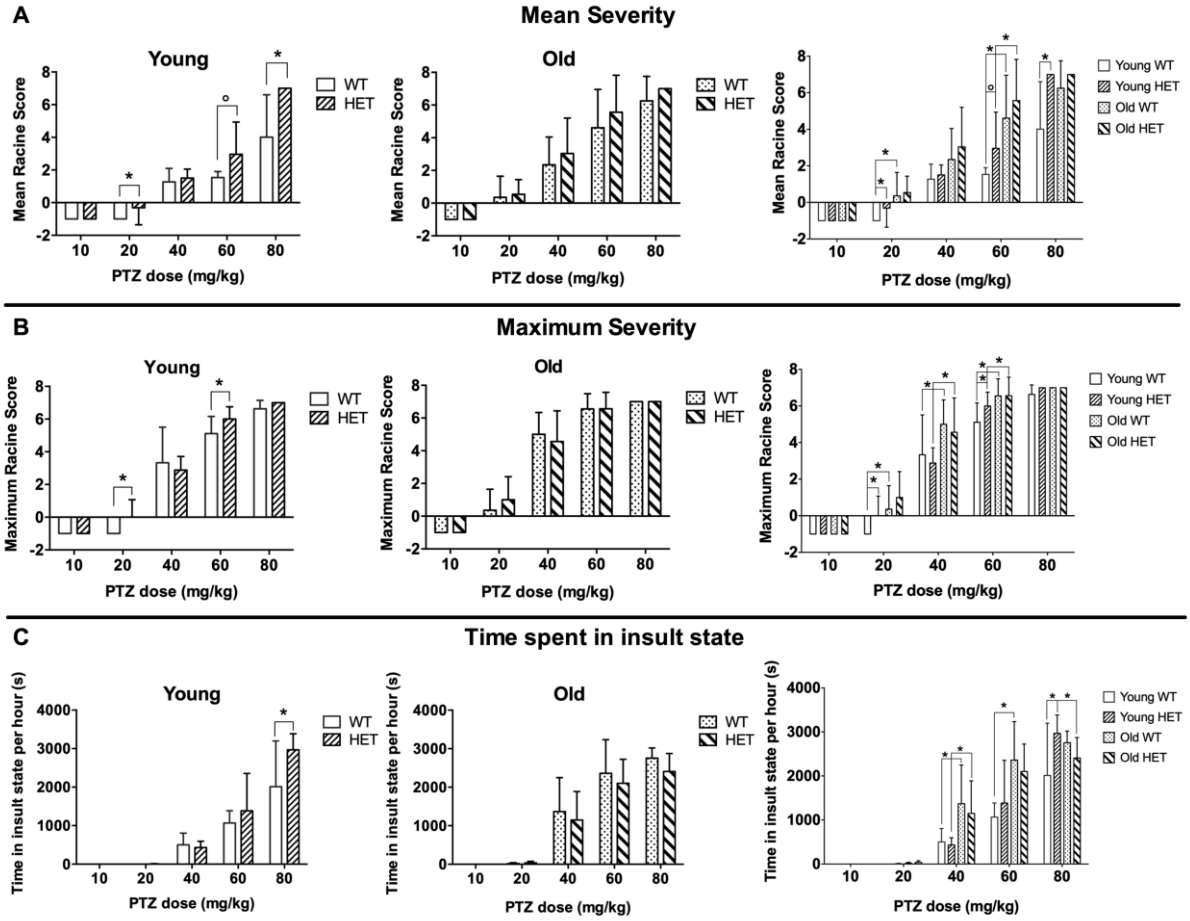

Figure 2.A. **Mean seizure severity.** Young HET mice had higher mean severity scores than WT littermates. Np significant genotype differences were observed in the old age group. A significant age component was observed, as old animals had higher mean seizure severity scores. **B. Maximum seizure severity.** Also higher maximal Racine scores were observed in young HET mice compared to WT animals, especially in the 20 and 60 mg/kg group. Old mice (both WT and HET) suffered on average more severe seizures than young mice. In addition, no genotype differences were observed in old animals **C. Time spent in insult state.** In the dose group of 80 mg/kg, young HET mice spent a longer time in seizure state compared to their WT littermates. Both old WT and HET mice resided longer in seizure state than young mice. The time spent in insult state in old HET animals also appeared to be lower than in young HET animals after a dose of 80 mg/kg and can probably be explained by the increased latency to seizures present in older animals. N = 163 (*Young*: 10 mg/kg: 6 WT + 5 HET, 20 mg/kg: 8 WT + 8 HET, 40 mg/kg: 9 WT + 8 HET, 60 mg/kg: 9 WT + 8 HET, 80 mg/kg: 8 WT + 8 HET; *Old*: 10 mg/kg: 9 WT + 9 HET, 20 mg/kg: 11 WT + 9 HET, 40 mg/kg: 10 WT + 9 HET, 60 mg/kg: 11 WT + 9 HET, 80 mg/kg: 4 WT + 5 HET).

* $p < 0.05$, ° $p \leq 0.05$, HET=heterozygote, WT=wild-type, PTZ=pentylenetetrazole.

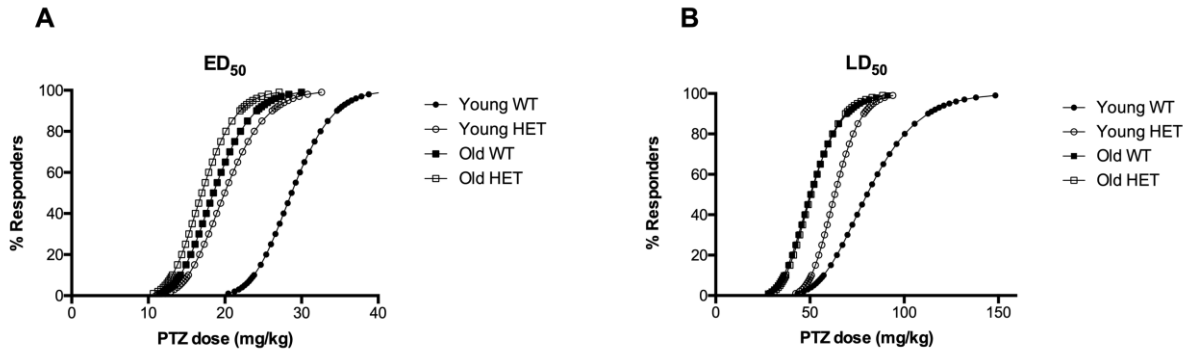

Figure 3. **ED_{50} and LD_{50} dose-response curves demonstrate reduced sensitivity of young wild-type mice. A.** The effective dose, at which 50% of the animals experienced an electrographically defined seizure, was highly elevated in young WT mice compared to the rest of the groups (Young WT: 28.7 mg/kg; Young HET: 20.0 mg/kg; Old WT: 18.5 mg/kg; Old HET: 17.0 mg/kg). **B.** Similarly, the lethal dose was obviously higher in young WT animals than in young HET animals. In old animals, this difference disappeared. Also, the age-related effect was clearly visible when comparing the LD_{50} values (Young WT: 80.3 mg/kg; Young HET: 63.2 mg/kg; Old WT: 50.2 mg/kg; Old HET: 50.6 mg/kg). N = 163 (*Young*: 10 mg/kg: 6 WT + 5 HET, 20 mg/kg: 8 WT + 8 HET, 40 mg/kg: 9 WT + 8 HET, 60 mg/kg: 9 WT + 8 HET, 80 mg/kg: 8 WT + 8 HET; *Old*: 10 mg/kg: 9 WT + 9 HET, 20 mg/kg: 11 WT + 9 HET, 40 mg/kg: 10 WT + 9 HET, 60 mg/kg: 11 WT + 9 HET, 80 mg/kg: 4 WT + 5 HET). HET=heterozygote, WT=wild-type, PTZ=pentylenetetrazole.

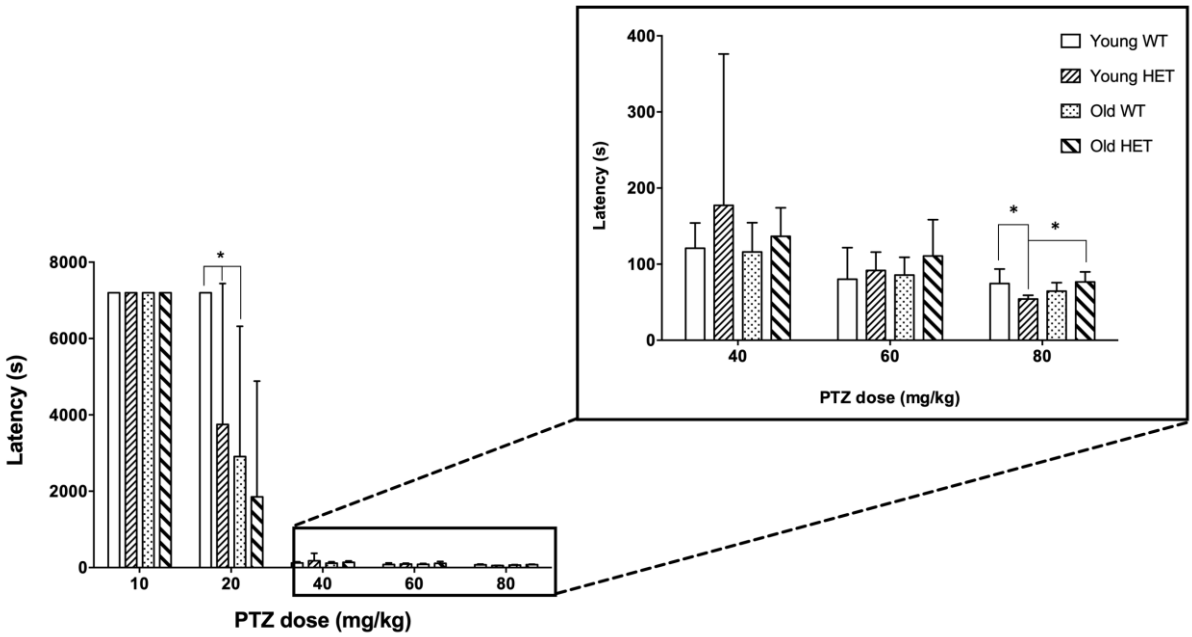

Figure 4. **Latency to first insult.** In the dose group of 80 mg/kg, 3-month-old HET mice had a shorter latency to first insult than their WT littermates. Age-related effects were also observed in the 80 mg/kg group, in which old HET mice had a longer latency than young HET mice. In the 20 mg/kg dose group, old WT animals and young HET both had a shortened latency to first insult compared to young WTs. N = 163 (*Young*: 10 mg/kg: 6 WT + 5 HET, 20 mg/kg: 8 WT + 8 HET, 40 mg/kg: 9 WT + 8 HET, 60 mg/kg: 9 WT + 8 HET, 80 mg/kg: 8 WT + 8 HET; *Old*: 10 mg/kg: 9 WT + 9 HET, 20 mg/kg: 11 WT + 9 HET, 40 mg/kg: 10 WT + 9 HET, 60 mg/kg: 11 WT + 9 HET, 80 mg/kg: 4 WT + 5 HET). * $p < 0.05$, HET=heterozygote, WT=wild-type, PTZ=pentylenetetrazole.

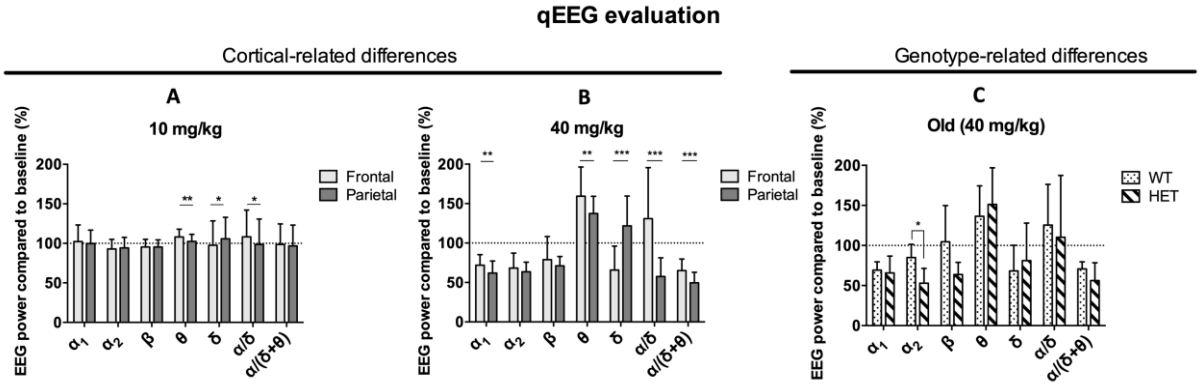

Figure 5. **qEEG evaluation demonstrates differences in frontal and parietal seizure manifestation. A.** In the dose group of 10 mg/kg, all EEG powerbands are located around baseline level (100%). Differences in theta, delta and alpha/delta power between frontal and parietal signals were observed. **B.** After administration of 40 mg/kg, a decrease in alpha and beta power is visible and an increase in theta power. Depending on the position of the electrode a rise or decline in delta power is observed. After a high dose of PTZ, the differences between frontal and parietal powerbands were more pronounced than after administration of a low dose. Highly significant differences were present between frontal and parietal regions in $alpha_1$, theta, delta, alpha/delta and alpha/(delta+theta) **C.** Significant genotype-related differences were only found in the frontal $alpha_2$ power spectrum, in which old HET animals had a more severe reduction than WT animals. 10 mg/kg: n = 18, 40 mg/kg: n = 19, Old (40 mg/kg): WT: n = 5, HET: n = 5. * $p < 0.05$, ** $p < 0.01$, *** $p < 0.001$, HET=heterozygote, WT=wild-type, PTZ=pentylenetetrazole.

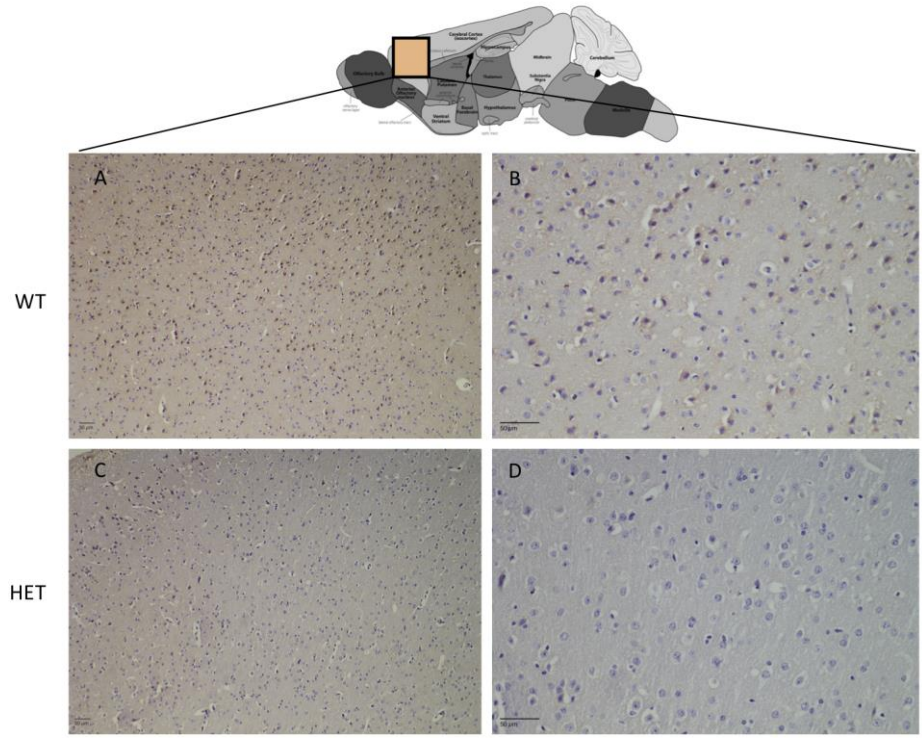

Figure 6. **GLT-1 immunoreactivity in frontal cortex of 3-month-old Tau58/4 mice.** Wild-type (WT) animals appear to have more GLT-1 glutamate transporters in the frontal cortex compared to heterozygous (HET) animals, as is demonstrated by an increased immunoreactivity (brown color packed around nuclei). **A.** Representative sagittal section of the frontal region of a 3-month-old WT stained with GLT-1 antibody. Brown color around nuclei indicates the presence of GLT-1 **B.** Magnified (2.5x) frontal region of 3-month-old WT animal (in 'A'). **C.** Representative slide of the frontal region of a HET Tau58/4 mouse, stained with GLT-1 antibody. Little immunoreactivity is present. **D.** Magnified image (2.5x) of the frontal region of the HET Tau58/4 animal (in 'C').

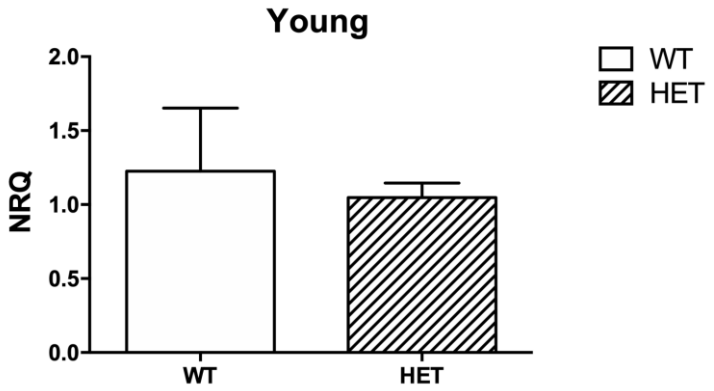

Figure 7. **GLT-1 mRNA levels in the left cortical hemisphere of 3-month-old Tau58/4 mice.** NRQs of WT (n = 5) versus HET (n = 5) animals were obtained using two normalization factors, including glyceraldehyde-3-phosphate dehydrogenase and beta-actin. HET=heterozygote; WT=wild-type;

Table 1: **Amount of animals included in the study and received doses per genotype and age.**

PTZ dose (mg/kg)	Young (3M)	Old (12-15M)
10	11 mice (6 WT + 5 HET)	18 mice (9 WT + 9 HET)
20	16 mice (8 WT + 8 HET)	20 mice (11 WT + 9 HET)
40	17 mice (9 WT + 8 HET)	19 mice (10 WT + 9 HET)
60	17 mice (9 WT + 8 HET)	20 mice (11 WT + 9 HET)
80	16 mice (8 WT + 8HET)	9 mice (4 WT + 5HET)

HET=heterozygote; WT = wild-type; PTZ=pentylenetetrazole; 3M=three months old; 12-15M=12 to 15 months old.

v